

Contents lists available at ScienceDirect

Petroleum Science

journal homepage: www.keaipublishing.com/en/journals/petroleum-science



Original Paper

Three-dimensional internal multiple elimination in complex structures using Marchenko autofocusing theory



Pei-Nan Bao a, b, *, Ying Shi a, Xin-Min Shang b, Hong-Xian Liang b, Wei-Hong Wang a

- ^a School of Earth Sciences, Northeast Petroleum University, Daqing, 163318, Heilongjiang, China
- ^b Geophysical Research Institute of Shengli Oilfield, Sinopec, Dongying, 257022, Shandong, China

ARTICLE INFO

Article history: Received 7 February 2024 Received in revised form 19 June 2024 Accepted 24 July 2024 Available online 26 July 2024

Edited by Meng-Jiao Zhou

Keywords:
Marchenko
Internal multiple elimination
Autofocusing
Three-dimensional seismic data

ABSTRACT

Internal multiples are commonly present in seismic data due to variations in velocity or density of subsurface media. They can reduce the signal-to-noise ratio of seismic data and degrade the quality of the image. With the development of seismic exploration into deep and ultradeep events, especially those from complex targets in the western region of China, the internal multiple eliminations become increasingly challenging. Currently, three-dimensional (3D) seismic data are primarily used for oil and gas target recognition and drilling. Effectively eliminating internal multiples in 3D seismic data of complex structures and mitigating their adverse effects is crucial for enhancing the success rate of drilling. In this study, we propose an internal multiple prediction algorithm for 3D seismic data in complex structures using the Marchenko autofocusing theory. This method can predict the accurate internal multiples of time difference without an accurate velocity model and the implementation process mainly consists of several steps. Firstly, simulating direct waves with a 3D macroscopic velocity model. Secondly, using direct waves and 3D full seismic acquisition records to obtain the upgoing and downgoing Green's functions between the virtual source point and surface. Thirdly, constructing internal multiples of the relevant layers by upgoing and downgoing Green's functions. Finally, utilizing the adaptive matching subtraction method to remove predicted internal multiples from the original data to obtain seismic records without multiples. Compared with the two-dimensional (2D) Marchenko algorithm, the performance of the 3D Marchenko algorithm for internal multiple prediction has been significantly enhanced, resulting in higher computational accuracy. Numerical simulation test results indicate that our proposed method can effectively eliminate internal multiples in 3D seismic data, thereby exhibiting important theoretical and industrial application value.

© 2025 The Authors. Publishing services by Elsevier B.V. on behalf of KeAi Communications Co. Ltd. This is an open access article under the CC BY-NC-ND license (http://creativecommons.org/licenses/by-nc-nd/

4.0/).

1. Introduction

Until now, most seismic imaging techniques still require primary reflection energy for their applications. To meet this requirement, multiples should be eliminated to avoid producing artifacts and misleading subsequent seismic interpretation and drilling (Weglein et al., 1997; Panos and Verschuur, 2000; Ikelle, 2006; Bao et al., 2021, 2022; Ijsseldijk et al., 2022). The western region of China is rich in oil/gas resources, but its geological characteristics are complex. The strong reflection interface (low coal seam) in the subsurface can generate internal multiples with strong

energy (Gan et al., 2018). The internal multiples exacerbate the blurring characteristics of deep geological wave groups, resulting in unclear geological structures and contact relationships. They restrict our understanding of internal geological structures and seriously affect oil/gas exploration and development in the northwest region. Additionally, the marine oil/gas resources are extremely abundant. However, multiples and primaries often overlap because of the rugged seabed structure, leading to poor imaging effects that directly affect the exploration and development deployment of offshore oil/gas fields. Compared with surface-related multiples, internal multiples are generated by stronger reflection sources and varied propagation types. Hence, the characteristics of internal multiples are more intricate, and the periodicity is poor. In deep seismic layers, the effective signal energy generally is weak. The differences in energy and velocity between

E-mail address: baopeinan123@126.com (P.-N. Bao).

^{*} Corresponding author.

multiples and primaries are also small, rendering identification and elimination challenging. It has remained difficult to find a completely effective method to solve the problem of internal multiples until now. Moreover, seismic data processing personnel frequently employ 2D technology to eliminate internal multiples in 3D seismic data, processing it line by line. However, 2D technology experiences difficulty in effectively matching the predicted multiple amplitudes with actual multiples in complex media and large travel time errors. Therefore, it is crucial to create a new 3D internal multiple elimination algorithm for seismic exploration.

Inspired by the Marchenko imaging method, Meles et al. (2015) exploited Marchenko autofocusing theory (Rose, 2002; Wapenaar, 2004; Wapenaar et al., 2012) and seismic interferometry to eliminate internal multiples. Singh et al. (2015) extended the Marchenko equation to retrieve Green's function, which includes primaries, internal multiples, and free-surface multiples. Therefore, we can retrieve the Green's function in the presence of a free surface. Furthermore, Meles et al. (2016) proposed a method for directly estimating primaries, which is based on the Marchenko reference plane reconstruction method and convolutional interferometry. This method avoids adaptive subtraction but necessitates estimation of the direct waves. Van der Neut and Wapenaar (2016) developed a scheme for eliminating internal multiples from measured acoustic fields by utilizing the modified Marchenko equation and implemented it in a one-dimensional (1D) numerical example. Da Costa Filho et al. (2017) applied the internal multiple elimination method to general elastic media based on the Marchenko method and convolutional interferometry. Thorbecke et al. (2017) detailed the implementation of the Marchenko method. Moreover, Zhang and Staring (2018) rewrote the Marchenko autofocusing internal multiple elimination scheme and proposed a new Marchenko multiple elimination (MME) method without velocity model information or adaptive subtraction. This method replaces the estimation of the two-way travel time surface with a fixed truncation for all traces. It only requires the input of seismic records, eliminating the need for macroscopic velocity models to estimate direct waves, and predicts all internal multiples during the iteration. Zhang et al. (2019) proposed transmission-compensated Marchenko multiple elimination based on the MME method. The approach can effectively eliminate internal multiples and compensate for the transmission loss of primaries during propagation. Based on Singh et al. (2015) and other preliminary research, Zhang and Slob (2019) further derived the Marchenko equation to retrieve the primaries from the acoustic surface-reflection response by eliminating the surface-related and internal multiples in one step. In another study, Zhang and Slob (2020) applied the MME method to a deep-water field data set from the Norwegian North Sea and achieved promising results. Elison et al. (2020) utilized the MME method to incorporate multi-dimensional energy conservation and terms based on the minimum phase principle, in order to accurately account for internal multiple scattering over both long and short periods. The results demonstrate that the "augmented" Marchenko method is superior, but the multidimensional minimum phase condition incorporated into the medium remains unclear. Wapenaar et al. (2021) employed a general mathematical framework to systematically investigate and discuss the reconstruction of the Marchenko baseline, Marchenko imaging, MME, and their interrelatedness. Additionally, He and Geng (2022) developed a novel scheme for predicting surface-related multiples by integrating the revised Marchenko equation with freesurface effects and convolutional seismic interferometry. Peng et al. (2023) improved the Marchenko method, which performs very well in settings with moderate lateral variations and effectively eliminates short-period multiples.

For the 3D Marchenko theory, Wapenaar et al. (2004) derived

the relationships between reflection and transmission responses in 3D nonhomogeneous media, which established the foundation for addressing the 3D Green's function. Wapenaar et al. (2013) employed the 3D Marchenko equation to retrieve the Green's function. Wapenaar (2013) derived a 3D Marchenko equation related to the single-sided reflection response of a 3D inhomogeneous medium to the field within the medium. Staring et al. (2018a) proposed an adaptive double-focusing method to remove multiples in 2D and 3D field data of the Santos Basin in Brazil. Jia et al. (2019) reformulated the Marchenko-type equations in a 3D cartesian coordinate system, which can be directly implemented in our 3D Marchenko algorithm. Brackenhoff et al. (2022) implemented the 3D Marchenko equations to retrieve accurate Green's functions within the medium and used these reflection data for imaging applications. The above studies are based on the Marchenko theory, and MME has demonstrated remarkable outcomes in eliminating multiples from field seismic data. However, only 2D internal multiple elimination methods have been developed based on the literature mentioned above. To address the high sampling density and large data volume encountered in seismic exploration, further research on 3D internal multiple elimination is necessary (Hokstad and Sollie, 2006). Based on the previous research, we utilize the dynamic characteristics of seismic waves and extend the 2D method to propose a 3D internal multiple elimination method that relies on the Marchenko autofocusing theory. This method can solve the problem of internal multiple elimination in 3D seismic

This study is organized as follows. After the introduction, we briefly review the 3D Marchenko autofocusing theory. Subsequently, we introduce 3D internal multiples construction and elimination. Finally, we utilize several synthetic experiments to validate the effectiveness of our approach and draw the corresponding conclusions.

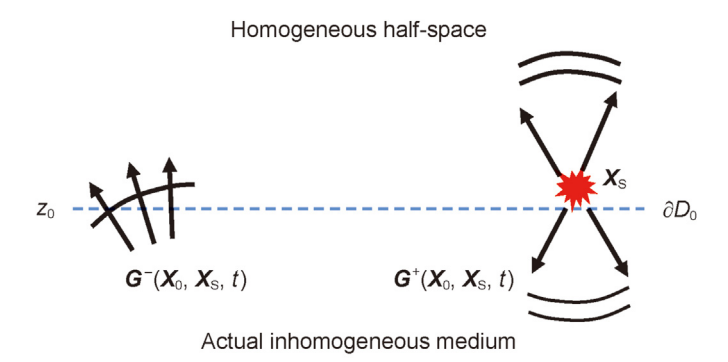
2. Method

2.1. Three-dimensional Marchenko autofocusing theory

We define Green's function $G(X,X_S,t)$ of the seismic source at X_S as the causal solution of the scalar wave equation in actual inhomogeneous media, according to Wapenaar et al. (2014a, 2014b).

$$\rho \nabla \cdot \left(\frac{1}{\rho} \nabla \mathbf{G}\right) - \frac{1}{\nu^2} \frac{\partial^2 \mathbf{G}}{\partial t^2} = -\rho \delta(\mathbf{X} - \mathbf{X}_{\mathrm{S}}) \frac{\partial \delta(t)}{\partial t}, \tag{1}$$

where $\mathbf{X} = (x, y, z)$ denotes spatial coordinates. Compared to 2D methods, there are more crossline variables. In 2D method, X =(x,z), which is different from the 3D method. The boundary ∂D_0 is defined as $z=z_0=0$. v=v(x) and $\rho=\rho(x)$ represent the propagation velocity and density of non-uniform media, respectively. T is the time. $X_S = X_{S,0}$ is selected just above ∂D_0 . ∂D_0 represents the acquisition surface where the observation system is located. Therefore, $\mathbf{X}_{S} = (x, y, z_0 - \varepsilon)$, $\varepsilon \rightarrow 0$. For convenience, we denote it as $X_{\rm H} = (x, y)$. The Green's function is decomposed into an upgoing wave field and a downgoing wave field, and they are coupled by the non-uniformity of the medium below the interface. The upgoing and downgoing Green's function components at the observation point **X** are represented by $G^+(X, X_S, t)$ and $G^-(X, X_S, t)$ (Fig. 1), respectively. Assuming that the one-way wavefields are pressurenormalized, the bidirectional Green's function can be defined as the superposition of the downgoing and upgoing fields, such as



 Z_1 ∂D_1 ∂C_2 ∂C_3 ∂C_4 ∂C_5 ∂C_5 ∂C_5 ∂C_6 ∂C_6

Fig. 1. The upgoing and downgoing components of Green's function of the wave equation in an actual inhomogeneous medium.

$$G(X, X_S, t) = G^{+}(X, X_S, t) + G^{-}(X, X_S, t),$$
(2)

where + and - represent downgoing and upgoing, respectively. The vertical derivative of the downgoing Green's function at the interface ∂D_0 (below the source point) is

$$\partial_z \mathbf{G}^+(\mathbf{X}, \mathbf{X}_{S}, t)|_{z=z_0} = -\frac{1}{2} \rho(\mathbf{X}_{S}) \delta(\mathbf{X}_{H} - \mathbf{X}_{S,H}) \frac{\partial \delta(t)}{\partial t}.$$
 (3)

The vertical derivative of the upgoing Green's function at the interface ∂D_0 is related to the pressure-normalized reflection response of the nonuniform medium beneath interface ∂D_0 ,

$$\partial_z \mathbf{G}^-(\mathbf{X}, \mathbf{X}_S, t)|_{z=z_0} = \frac{1}{2} \rho(\mathbf{X}_0) \frac{\partial \mathbf{R}(\mathbf{X}_S, \mathbf{X}_0, t)}{\partial t},$$
 (4)

where R represents the reflection response of downgoing waves below the depth level z=0 in the medium.

We define the focusing function $f_1(X,X_V,t)$ and $f_2(X,X_S,t)$ in the reference medium, as shown in Fig. 2 (Slob et al., 2014; Wapenaar et al., 2014a). The reference medium is the same as the actual medium above the depth ∂D_i , and no reflection is observed below the depth ∂D_i . Here, $X_V = (X_{V,H},z_i)$ is the focusing point, $X_{V,H}$ represents a point positioned horizontally on the interface ∂D_i , and X represents any observation point in the medium. Similar to Eq. (2), the focusing function can be written as the sum of pressure-normalized downgoing focusing function $f_1^+(X,X_V,t)$ and upgoing focusing function $f_1^-(X,X_V,t)$ components at the observation point (coupled with each other),

$$\mathbf{f}_{1}(\mathbf{X}, \mathbf{X}_{V}, t) = \mathbf{f}_{1}^{+}(\mathbf{X}, \mathbf{X}_{V}, t) + \mathbf{f}_{1}^{-}(\mathbf{X}, \mathbf{X}_{V}, t). \tag{5}$$

The focusing function $\mathbf{f}_1(\mathbf{X}, \mathbf{X}_V, t)$ focuses at $\mathbf{X}_H = \mathbf{X}_{V,H}$ at depth level ∂D_i and continues into the nonreflective reference half-space as a divergent downgoing field $\mathbf{f}_1^+(\mathbf{X}, \mathbf{X}_V, t)$. Referring to Eq. (3), the focusing function can be written as

$$\partial_z \boldsymbol{f}_1^+(\boldsymbol{X}, \boldsymbol{X}_{\mathrm{V}}, t)|_{z=z_i} = -\frac{1}{2} \rho(\boldsymbol{X}_{\mathrm{V}}) \delta(\boldsymbol{X}_{\mathrm{H}} - \boldsymbol{X}_{\mathrm{V},\mathrm{H}}) \frac{\partial \delta(t)}{\partial t}.$$
 (6)

Similarly, the focusing function $f_2(X, X_S, t)$ can be written as the sum of pressure-normalized downgoing and upgoing focusing

function components,

$$\mathbf{f}_{2}(\mathbf{X}, \mathbf{X}_{S}, t) = \mathbf{f}_{2}^{+}(\mathbf{X}, \mathbf{X}_{S}, t) + \mathbf{f}_{2}^{-}(\mathbf{X}, \mathbf{X}_{S}, t). \tag{7}$$

The focusing function $f_2(X,X_S,t)$ focuses at $X_H=X_{V,H}$ at depth level ∂D_0 and continues into the homogeneous half-space $z\leq z_i$ as a divergent downgoing field. Similar to Eq. (3), the focusing function can be written as

$$\partial_{z} \boldsymbol{f}_{2}^{-}(\boldsymbol{X}, \boldsymbol{X}_{V}, t)|_{z=z_{0}} = \frac{1}{2} \rho(\boldsymbol{X}_{V}) \delta(\boldsymbol{X}_{H} - \boldsymbol{X}_{S,H}) \frac{\partial \delta(t)}{\partial t}.$$
 (8)

At depths ∂D_0 and ∂D_i , the unidirectional focusing function is interrelated,

$$f_1^+(X_S, X_V, t) = f_2^-(X_V, X_S, t),$$
 (9)

and

$$-\boldsymbol{f}_{1}^{-}(\boldsymbol{X}_{S},\boldsymbol{X}_{V},-t) = \boldsymbol{f}_{2}^{+}(\boldsymbol{X}_{V},\boldsymbol{X}_{S},t). \tag{10}$$

The one-way focusing function at depth ∂D_i (Fig. 2), the focusing function at depth ∂D_0 , and the reflection response at depth ∂D_0 are interrelated. Therefore, we can obtain

$$\mathbf{G}^{-}(\mathbf{X}_{V}, \mathbf{X}_{S}, t) = \int_{\partial D_{0}} d\mathbf{X}_{0} \int_{-\infty}^{t} \mathbf{R}(\mathbf{X}_{S}, \mathbf{X}_{0}, t - t') \mathbf{f}_{1}^{+}(\mathbf{X}_{0}, \mathbf{X}_{V}, t') dt'$$
$$-\mathbf{f}_{1}^{-}(\mathbf{X}_{S}, \mathbf{X}_{V}, t), \tag{11}$$

$$\begin{aligned} \boldsymbol{G}^{+}(\boldsymbol{X}_{V}, \boldsymbol{X}_{S}, t) &= -\int_{\partial D_{0}} d\boldsymbol{X}_{0} \int_{-\infty}^{t} \boldsymbol{R}(\boldsymbol{X}_{S}, \boldsymbol{X}_{0}, t - t') \boldsymbol{f}_{1}^{-}(\boldsymbol{X}_{0}, \boldsymbol{X}_{V}, -t') dt' \\ &+ \boldsymbol{f}_{1}^{+}(\boldsymbol{X}_{S}, \boldsymbol{X}_{V}, -t), \end{aligned} \tag{12}$$

where the upper limit of time integration t'=t is obtained from the causal relationship of reflection response. The integral over the acquisition surface ∂D_0 enables us to parallelize over pairs of focal points. This is a significant advantage when applying the method to massive 3D data (Staring et al., 2018b).

Based on the causality of Green's function, the expressions on the left side of Eqs. (11) and (12) are equal to zero before the first arrival. Hence,

$$\boldsymbol{f}_{1}^{-}(\boldsymbol{X}_{S}, \boldsymbol{X}_{V}, t) = \int_{\partial D_{0}} d\boldsymbol{X}_{0} \int_{-\infty}^{t} \boldsymbol{R}(\boldsymbol{X}_{S}, \boldsymbol{X}_{0}, t - t') \boldsymbol{f}_{1}^{+}(\boldsymbol{X}_{0}, \boldsymbol{X}_{V}, t') dt'$$
(13)

$$\boldsymbol{f}_{1}^{+}(\boldsymbol{X}_{S},\boldsymbol{X}_{V},-t) = \int_{\partial D_{0}} \mathrm{d}\boldsymbol{X}_{0} \int_{-\infty}^{t} \boldsymbol{R}(\boldsymbol{X}_{S},\boldsymbol{X}_{0},t-t') \boldsymbol{f}_{1}^{-}(\boldsymbol{X}_{0},\boldsymbol{X}_{V},-t') \mathrm{d}t', \tag{14}$$

where the complex conjugate of the direct wavefield $G_d(X_S, X_V, -t)$ between the virtual source point and the surface receiver point is used as the initial value of the focusing function $f_1^+(X_S, X_V, t)$ for the traveling wave, so

$$\mathbf{f}_{1,0}^{+}(\mathbf{X}_{S},\mathbf{X}_{V},t) = \mathbf{G}_{d}(\mathbf{X}_{S},\mathbf{X}_{V},-t). \tag{15}$$

2.2. Three-dimensional internal multiples construction and elimination

We insert Eq. (15) into Eq. (13) to update the upgoing focusing

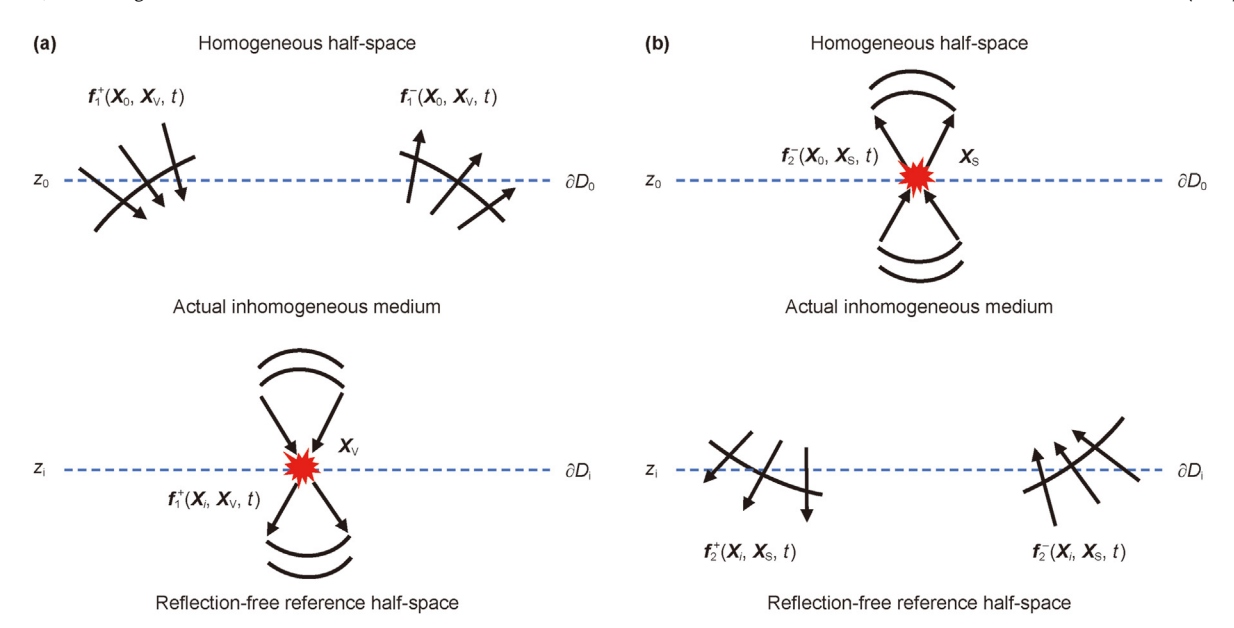


Fig. 2. The upgoing and downgoing components of focus function of the three-dimensional wave equation in reference medium. **(a)** The upgoing and downgoing components of focus function f_1 ; **(b)** the upgoing and downgoing components of focus function f_2 .

function value. Subsequently, we insert the updated upgoing focusing function value into Eq. (14) to update the downgoing focusing function value. We repeat this process until the energy converges to obtain the final upgoing and downgoing focusing function. We substitute the focused upgoing and downgoing focusing functions into Eqs. (11) and (12) to obtain the upgoing and downgoing Green's functions between the virtual source point and the surface. Internal multiples can be constructed that are related to the layer where the virtual source point is located by using the obtained upgoing and downgoing Green's functions and combining them through convolution operations. Fig. 3(b) illustrates how to use convolutional interferometry to reconstruct primaries and internal multiples in 3D space. From Fig. 3(a), one of the components for constructing primary reflections must use direct waves. On the contrary, if the downgoing Green's function with the first arrival part or upgoing Green's function with the first primaries are removed, the constructed new reflections are internal multiples of this relevant layer. For operational convenience, we use the downgoing Green's function excluding arrival parts and complete the upgoing Green's function wave field to construct internal multiples. The construction formula is shown in Eq. (16).

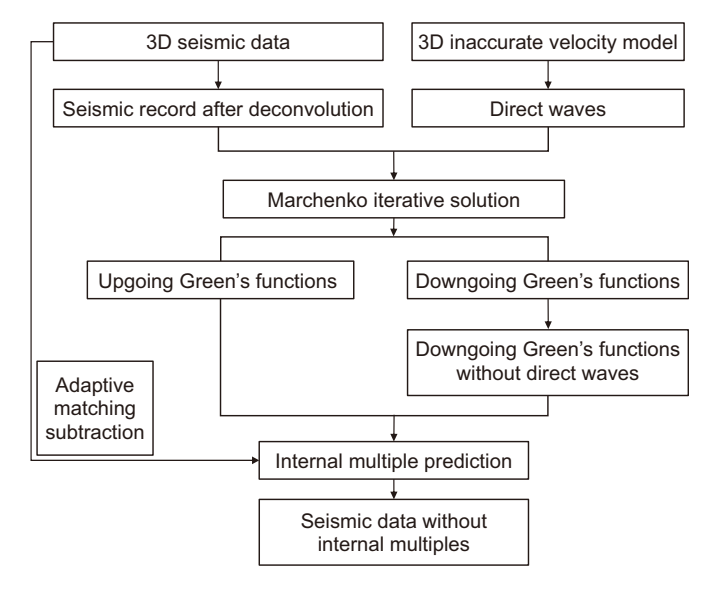


Fig. 4. 3D Marchenko internal multiple elimination flowchart.

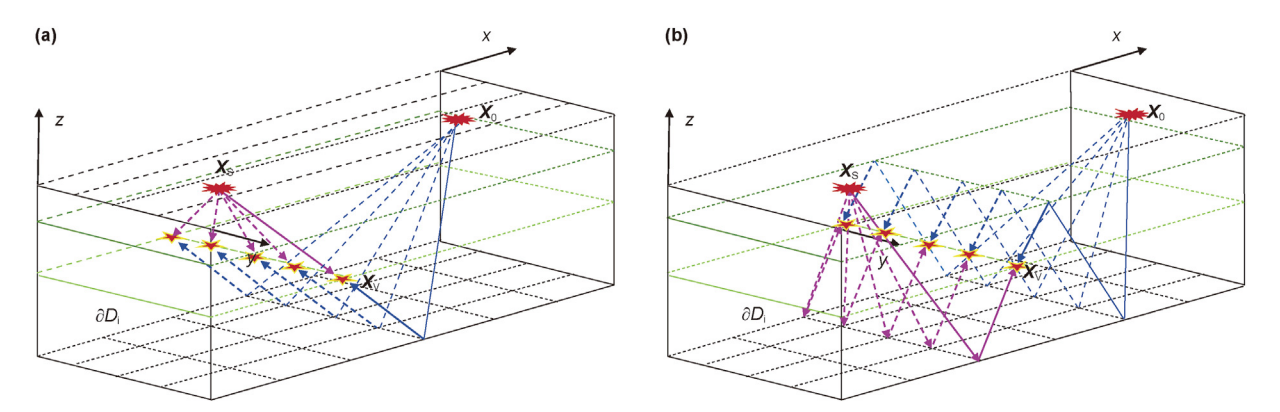


Fig. 3. Principle to construct primaries and internal multiples. (a) Using downgoing Green's function and the direct component of upgoing Green's function to construct primaries; (b) using downgoing and upgoing Green's function for cutting off the direct part to construct internal multiples.

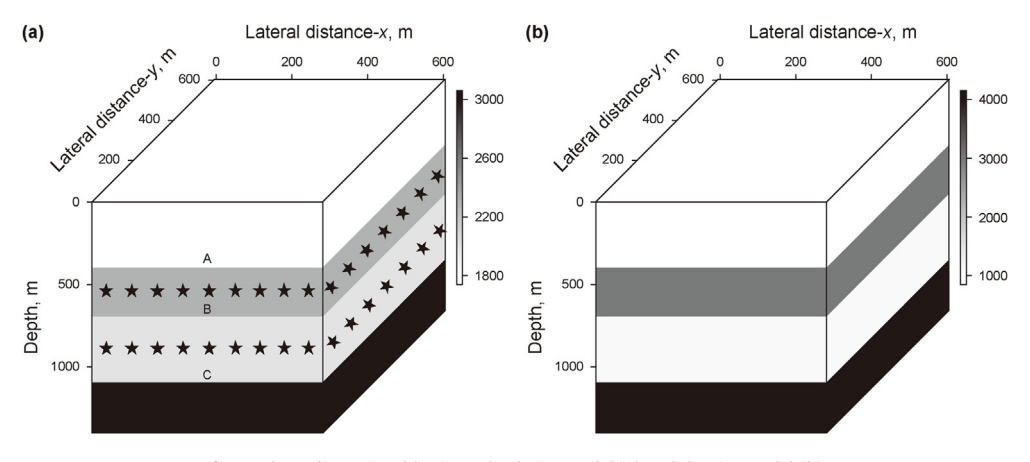


Fig. 5. Three-dimensional horizontal velocity model (a) and density model (b).

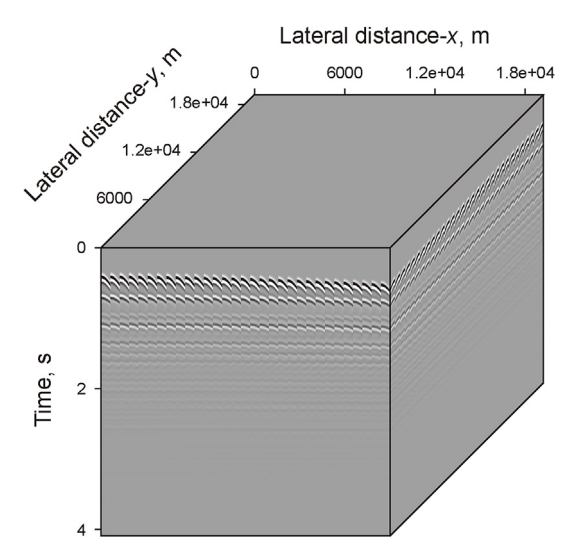


Fig. 6. 3D seismic records.

$$\boldsymbol{M}_{V}(\boldsymbol{X}_{S},\boldsymbol{X}_{0},t) = \int_{\partial D_{0}} d\boldsymbol{X} \int_{t}^{\infty} \boldsymbol{G}^{-}(\boldsymbol{X}_{V},\boldsymbol{X}_{S},t') \boldsymbol{G}_{d}^{+}(\boldsymbol{X}_{V},\boldsymbol{X}_{S},t') dt',$$

$$\tag{16}$$

where $\mathbf{M}_{\rm V}(\mathbf{X}_{\rm S},\mathbf{X}_{\rm 0},t)$ is the predicted internal multiples for the virtual source point V.

The 3D Marchenko algorithm method contains four key points. The first key point is using a macroscopic underground velocity model to estimate direct waves. The second key point is combing direct waves and autofocusing theory to generate upgoing and downgoing Green's functions of relevant discrete virtual source points along the selected subsurface. The third key point is employing the calculated upgoing and downgoing Green's functions to predict internal multiples through convolution. The fourth key point is using adaptive subtraction to eliminate the predicted internal multiples from the original data. Because the phase and amplitude of 3D internal multiples predicted by the Marchenko method are incorrect. Therefore, an adaptive matching subtraction algorithm is necessary to remove internal multiples from the observed data. The process is shown in Fig. 4. We use a multichannel adaptive matching method for subtraction (Wang, 2003).

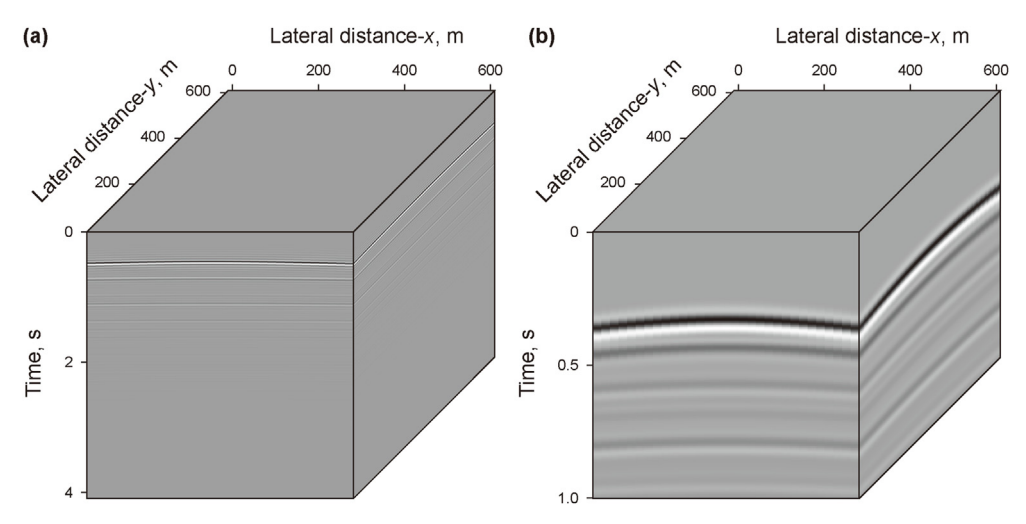


Fig. 7. Input seismic data for the internal multiple elimination method using the Marchenko autofocusing method. (a) Shot record; (b) transmission response.

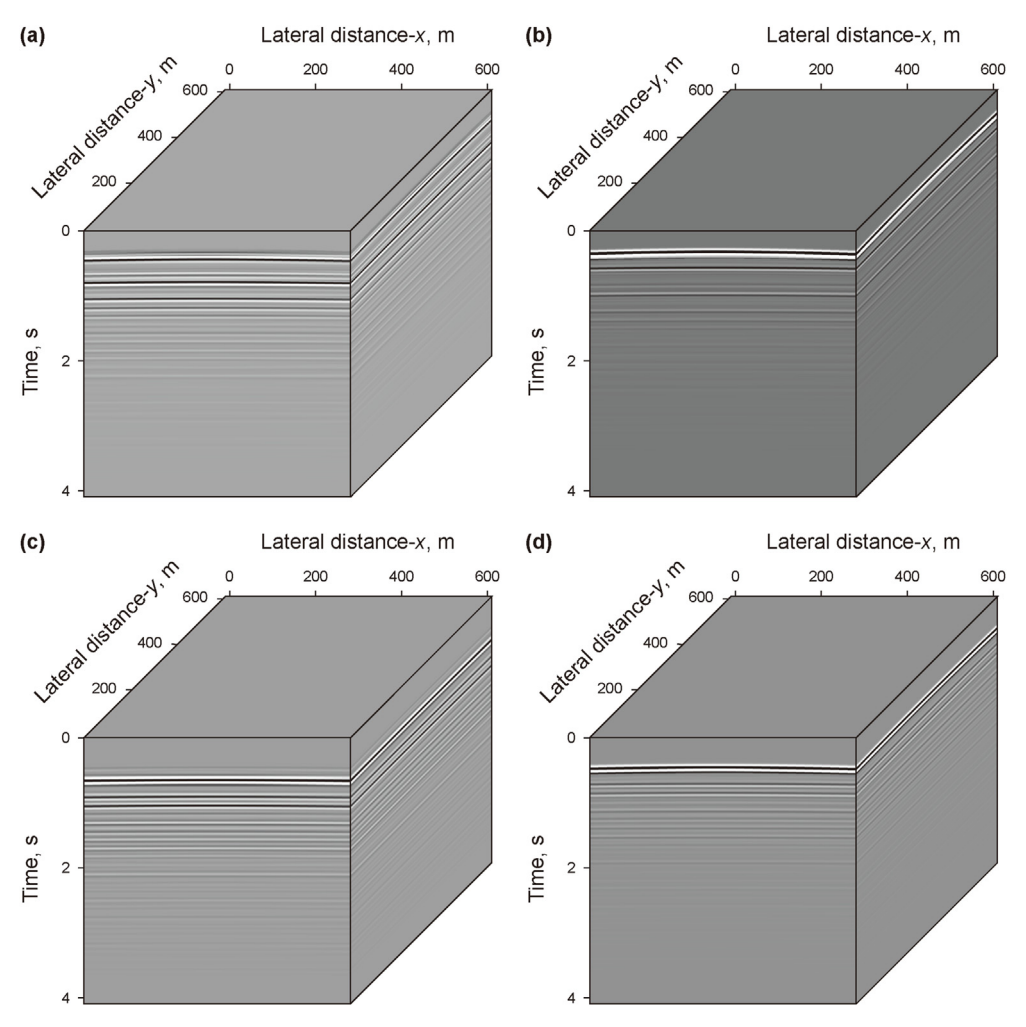


Fig. 8. Upgoing and downgoing Green's functions. (a) Upgoing Green's function when virtual source point is placed at 600 m; (b) downgoing Green's function when virtual source point is placed at 600 m; (c) upgoing Green's function when virtual source point is placed at 900 m; (d) downgoing Green's function when virtual source point is placed at 900 m.

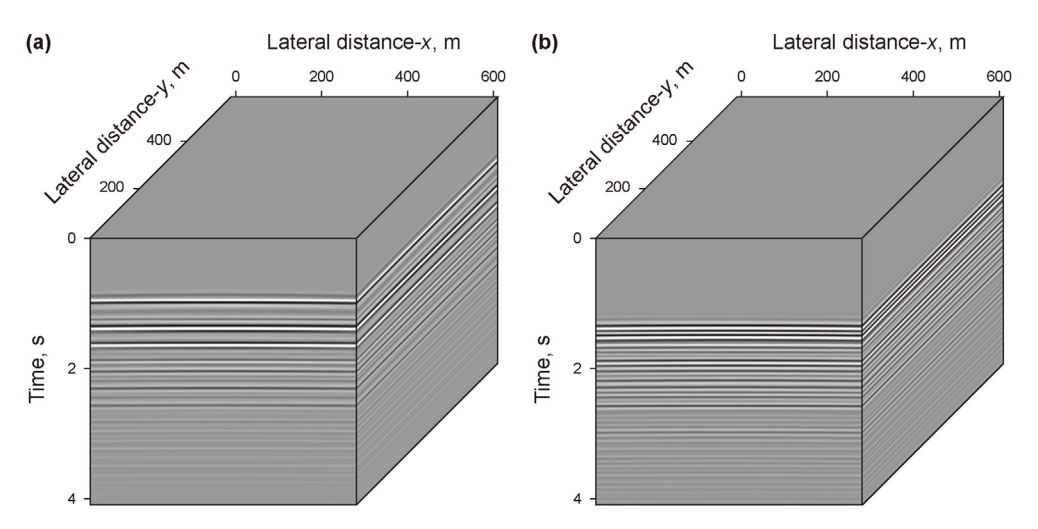


Fig. 9. Predicted internal multiples. (a) Predicted internal multiples when the virtual source point is placed at 600 m; (b) predicted internal multiples when the virtual source point is placed at 900 m.

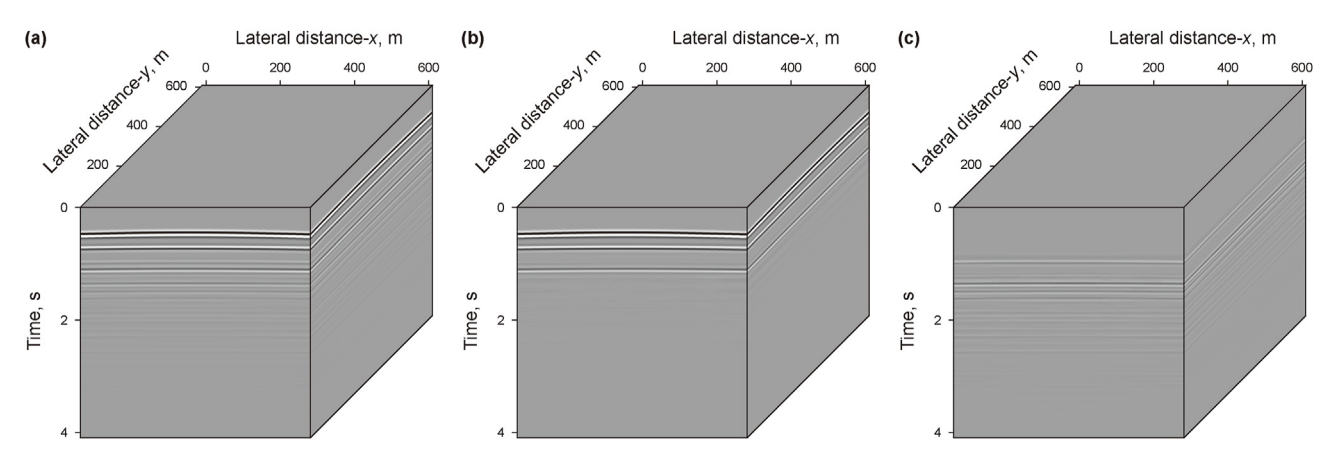


Fig. 10. Shot gather without internal multiples. (a) Raw shot record; (b) results with all internal multiples eliminated; (c) the difference between Fig. 10(a) and 10(b).

3. Examples

3.1. Horizontal layer model example

To test the effectiveness of the 3D Marchenko internal multiple elimination method, firstly, we use a 3D simple horizontal layered model for testing, as depicted in Fig. 5(a). Fig. 5(b) is density model. The model size is $600 \times 600 \times 1400$ m³. We use a fixed-spread acquisition with a grid of 961 sources and receivers of 20 m spacing in a square shape. The seismic data is modeled using a 15 Hz Ricker wavelet. The reflection time of seismic records is 4.902 s, and the time sampling interval is 4 ms. The modeled reflection responses are presented in Fig. 6, and all direct waves are cut off. When solving the Green's function, we input seismic records and transmission response for multiple convolution operations, which results in wavelet effects. In order to avoid wavelet effects, the reflection data must be deconvolved for the wavelet (Mildner et al., 2017). The result of this deconvolution is the reflection response of a zero-phase wavelet with a flat spectrum between the frequencies f_{min} and f_{max} . A wavelet similar to the sinc wave that has a flat frequency spectrum of amplitude. Hence, in numerical simulation examples, to prevent wavelet deconvolution, the sinc wave is employed as the source during the forward modeling. The source wavelet with a flat frequency spectrum between $f_{min} = 5$ Hz and $f_{max} = 30$ Hz is described in Fig. 7(a). Fig. 7(b) shows the transmission response, recorded at the surface for a

source at a 900 m depth, as input seismic data.

Fig. 8(a)-(d) show the upgoing and downgoing Green's functions, which are constructed by placing the virtual source point at depths of 600 and 900 m, as indicated by the five-pointed star in Fig. 5(a), respectively. To construct the related layer of internal multiples, we insert downgoing G^+ without first arrival events and upgoing **G**⁻ components of the Green's functions into the internal multiples reconstruction, as expressed in Eq. (16) (Fig. 9). Compared with internal multiples in actual seismic records, the reconstructed internal multiples have consistent phase and time differences; however, differences in amplitude are observable. Adaptive matching subtraction is required to match the internal multiples present in the original seismic records. The results of internal multiple elimination achieved through adaptive matching are depicted in Fig. 10. Fig. 10(a) displays the original shot record of the 481th shot, while Fig. 10(b) illustrates the shot record following the elimination of internal multiples associated with interfaces A and B. It means the internal multiples are constructed when the virtual source points are placed at 600 and 900 m depth, all of which have been eliminated. Fig. 10(c) displays the differences between shot record with multiples and the result of multiple elimination. All the internal multiples in the seismic records are effectively eliminated.

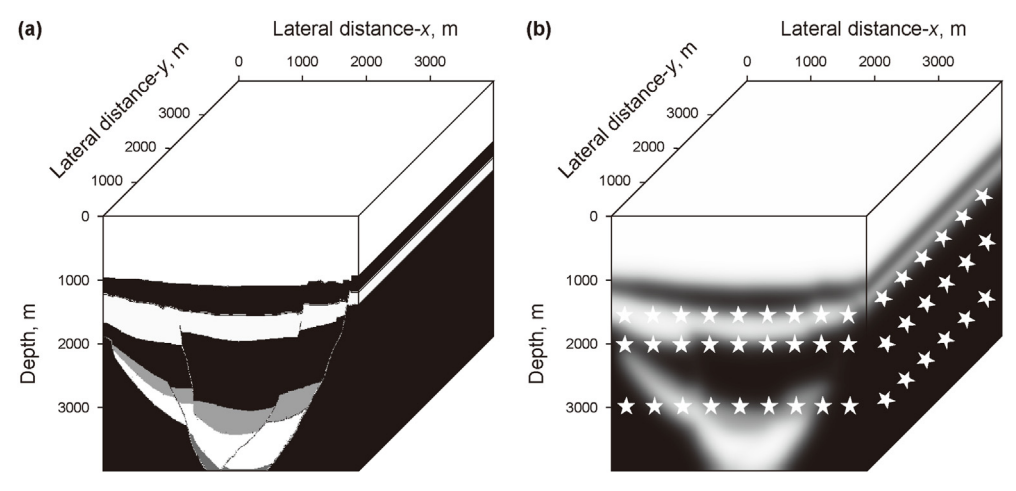


Fig. 11. 3D faulted basins velocity model. (a) Velocity model; (b) inaccurate velocity model.

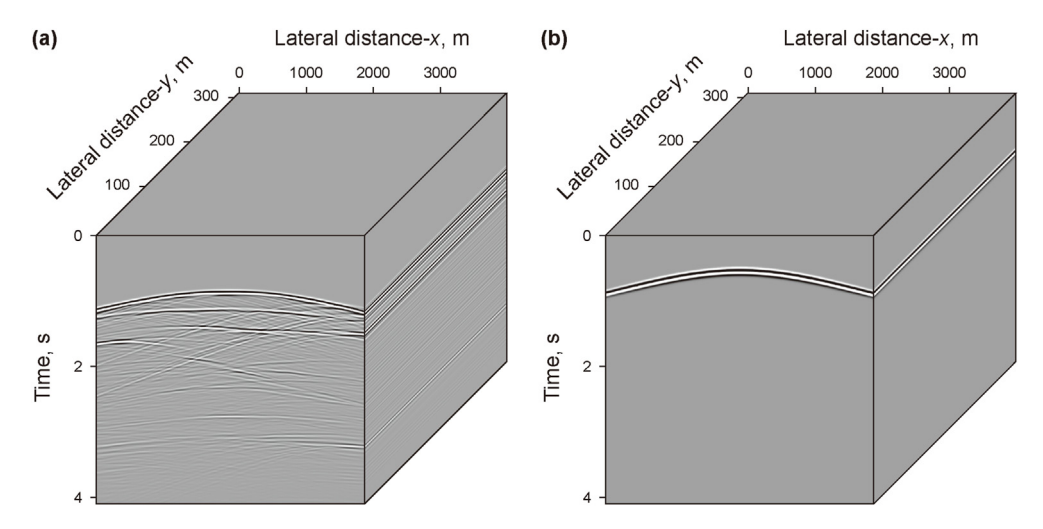


Fig. 12. Input seismic data for 3D Marchenko autofocusing internal multiple elimination method. (a) Modeled shot record; (b) transmission response.

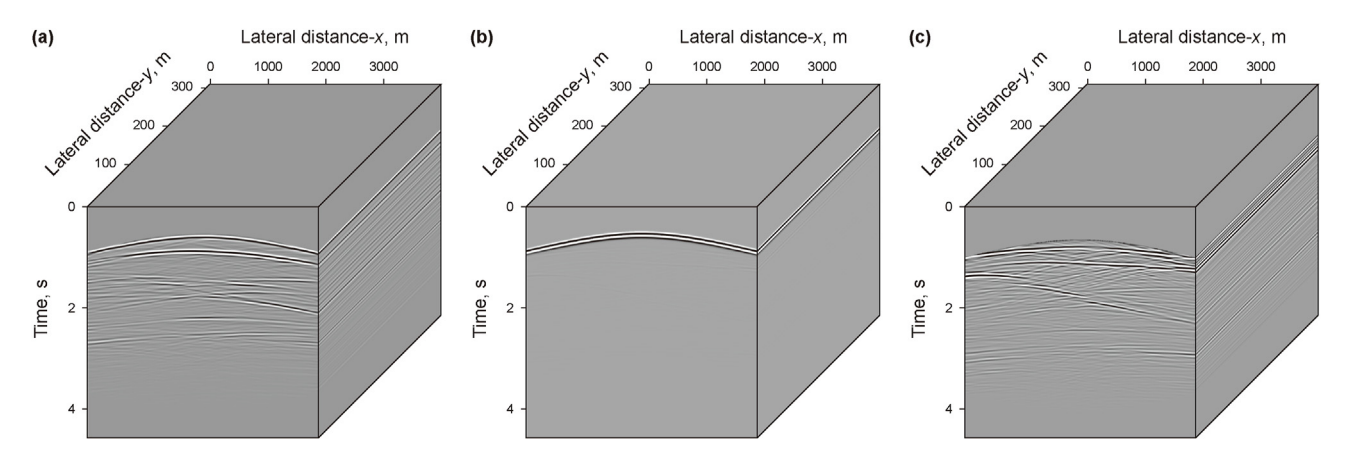


Fig. 13. Upgoing and downgoing Green's functions. (a) Upgoing Green's function when virtual source point is placed at 1500 m; (b) downgoing Green's function when virtual source point is placed at 1500 m; (c) downgoing Green's function without first arrival wave.

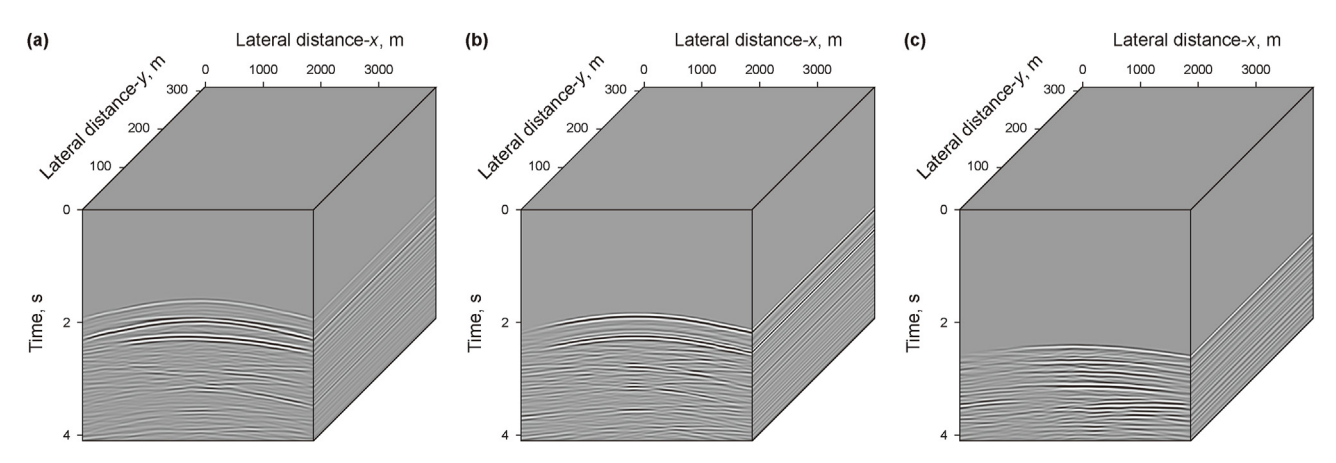


Fig. 14. Predicted internal multiples. (a) Predicted internal multiples when virtual source point is placed at 1500 m; (b) predicted internal multiples when virtual source point is placed at 2000 m; (c) predicted internal multiples when virtual source point is placed at 3000 m.

3.2. Complex model example

To further test the effectiveness of the 3D Marchenko internal multiple elimination method, we have chosen a complex 3D fault basin geological model for measurement, as depicted in Fig. 11(a).

Fig. 11(b) represents a smoothed velocity model based on Fig. 11(a), with an error margin of up to 50%. This model serves as a macroscopic (inaccurate) velocity model for forwarding initial arrival events of transmission response. The model size is $4000 \times 4000 \times 4000$ m³. It is modeled using a zero-phase Ricker

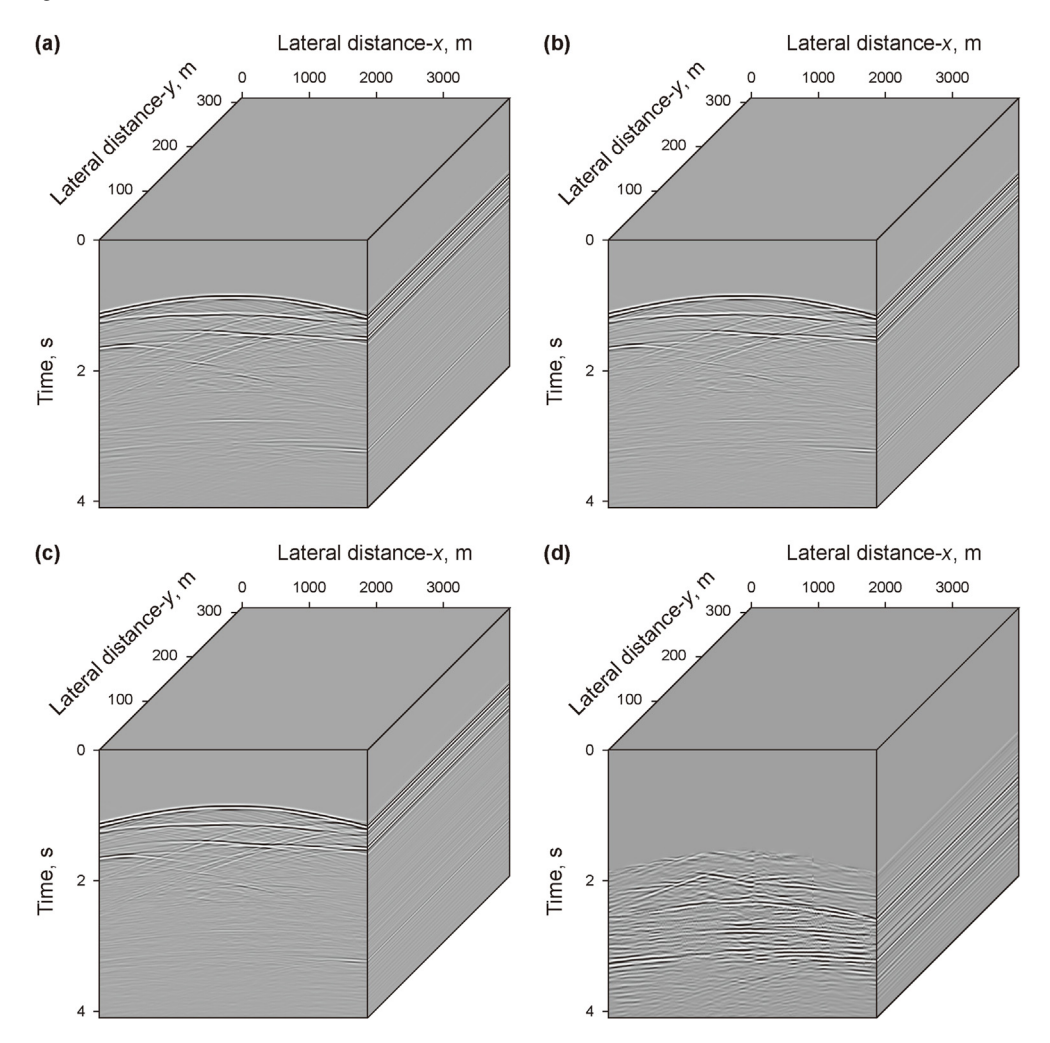


Fig. 15. Shot gather without internal multiples. (a) Results when virtual source point is placed at 1500 m; (b) results when virtual source point is placed at 2000 m; (c) results when virtual source point is placed at 3000 m; (d) the difference between Figs. 12(a) and 15(c).

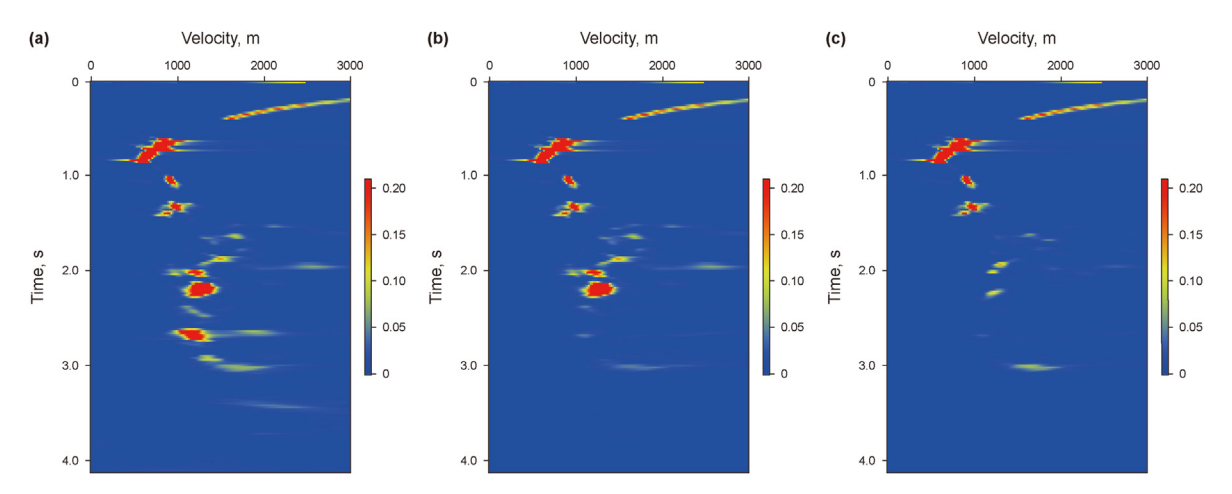


Fig. 16. Velocity spectrum. (a) Velocity spectrum of shot gather; (b) velocity spectrum without internal multiples when virtual source point is placed at 1500 m; (c) velocity spectrum without all internal multiples.

source wavelet with a peak frequency of 25 Hz. We simulate 16 survey lines, with 200 shots per survey line and 3200 receivers per shot, taking into account data quantity and computational complexity. The spacing between sources and receivers is 20 m. The

reflection time of seismic records is 4.1 s, and the time sampling interval is 4 ms. All direct waves have been eliminated. In the simulated data, Fig. 12(a) displays one of the shot records, which Fig. 12(b) exhibits the transmission response recorded at the

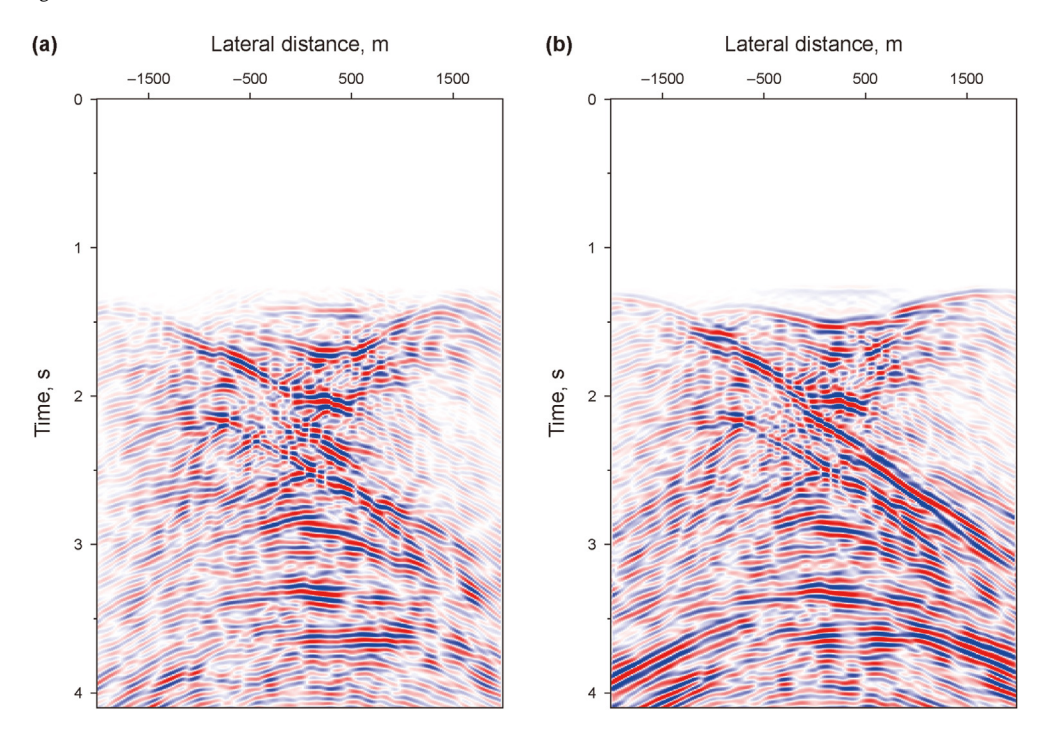


Fig. 17. Zero-offset of predicted internal multiples. (a) Zero-offset of predicted internal multiples using 2D Marchenko autofocusing method; (b) zero-offset of predicted internal multiples using 3D Marchenko autofocusing method.

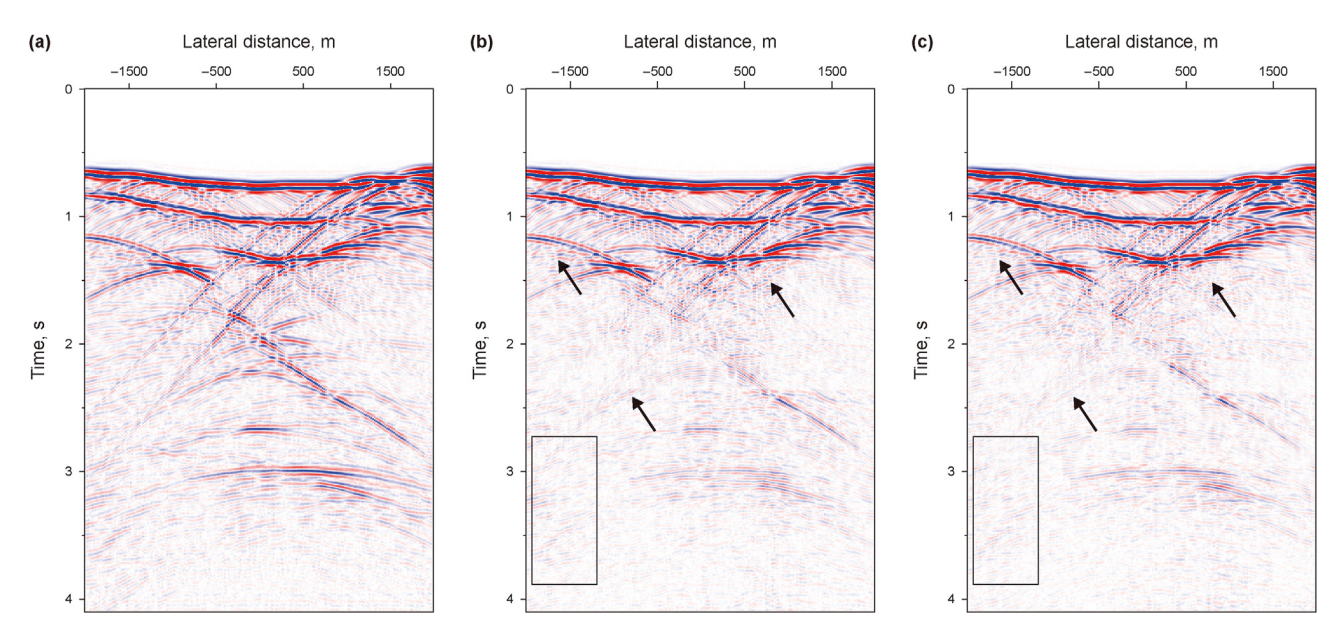


Fig. 18. Zero-offset data with internal multiple elimination. (a) Zero-offset data with internal multiples; (b) zero-offset data without internal multiples using 2D Marchenko autofocusing method; (c) zero-offset data without internal multiples using 3D Marchenko autofocusing method.

surface for a source positioned at a depth of 1000 m with in the macroscopic velocity model. We used the modeled transmission response and wavelet processed seismic records to derive Green's function field and construct internal multiples for relevant layers. In field seismic data processing, a macroscopic velocity model can be obtained by analyzing the velocity of seismic records. Subsequently, we simulate the transmission response between virtual source points and surface receiving points, utilizing the obtained macroscopic velocity model.

Fig. 13 illustrates the upgoing and downgoing Green's functions derived from positioning the virtual source point at 1500 m within

the smoothed velocity model, along with the downgoing Green's functions subsequent to the elimination of the first arrival wave, respectively. Fig. 14 demonstrates the predicted internal multiples when the virtual source point is placed at 1500, 2000, and 3000 m, respectively, as indicated in Fig. 11(b). Fig. 15 shows the results of the internal multiple eliminations. Most of the internal multiples have been removed and effectively protect the primary. Fig. 16 exhibits the velocity spectrum. Fig. 16(a) depicts the velocity spectrum of the original data, while Fig. 16(b) represents the velocity spectrum after eliminating internal multiples through the placement of a placing the virtual source at 1500 m. Fig. 16(c) shows

the velocity spectrum after the removal of all internal multiples, providing a more intuitive visualization of the effectiveness of multiple elimination.

To observe the effectiveness of 2D and 3D methods in predicting multiples, we superimpose the predicted internal multiples of each horizon using both methods, as depicted in Fig. 17. Fig. 17(a) displays the predicted multiples using a 2D method, while Fig. 17(b) shows the predicted multiples using a 3D method. Fig. 18 demonstrates zero-offset data with internal multiples and zero-offset data without internal multiples, utilizing both 2D and 3D Marchenko autofocusing methods. The result using 3D Marchenko method is more accurate than 2D Marchenko method. Especially the positions indicated by the black arrows and within the black box.

4. Discussion

Multiples are a common type of coherent noise. When the energy of multiples is strong, the amplitude, frequency, and phase of primaries will be distorted, leading to degradation in the quality of the image. Therefore, they should be removed. The research on multiple eliminations based on wave theory and dynamic characteristics mostly employs 2D seismic data (Kelamis and Verschuur, 2000). The multiple eliminations in 2D seismic data have developed into a series of relatively mature technologies. In practical applications, seismic data processors often directly apply 2D algorithms to 3D seismic data (Staring et al., 2021). This 2D assumption method for predicting and eliminating multiples in 3D data fails to take into the characteristics of underground interface dip angle. amplitude, and phase difference of seismic wave propagation in both 3D and 2D data, especially in complex geological structures. Therefore, conventional 2D internal multiple elimination methods are often unable to effectively predict complex 3D geological structures. Hence, ensuring the accuracy of multiple elimination results is challenging. The 3D algorithm for surface-related multiple eliminations has matured and been applied to industrial production, significantly enhancing the accuracy of 3D marine seismic data imaging (Baumstein and Hadidi, 2006; Dragoset et al., 2010). Moreover, similar to the surface-related multiples, the propagation of internal multiples is a 3D spatial function in practical situations. However, the depth and breadth of research on internal multiples are substantially lower compared to studies focusing on surfacerelated multiples. The main reason is that the generation mechanism of internal multiples is unclear; thus, predicting and eliminating them is challenging.

Based on the 2D Marchenko internal multiple elimination method (Thorbecke et al., 2021), we propose a fully 3D internal multiple elimination approach. This method conforms to the field seismic data and the real characteristics of underground media, thereby enhancing the accuracy and effectiveness of internal multiple eliminations. Furthermore, the data volume of 3D seismic data is usually large. Taking into account computational efficiency, we have only established 16 receivers in the crossline direction within the complex model. In the inline direction, the internal multiples are eliminated, effectively preserving primaries in the original seismic data. However, in the crossline direction, most multiples are eliminated, albeit the presence of residual multiples. The main reason for this issue is the scarcity of shots in the crossline direction (Fig. 15). When the crossline direction has the same or similar number of sources and receivers as the inline direction, the multiple elimination effect will be equivalent to that in the inline direction (Fig. 10(b)).

The Marchenko method for eliminating multiples is mainly divided into three parts: (1) simulating transmission response; (2) solving the upgoing and downgoing Green's function; (3) internal multiple prediction and elimination. Thus, for one shot in

horizontal layer model, the time of transmission wave forward modeling is approximately 61.87 s; the time for iterating 8 times to solve the upgoing and downgoing Green's functions is 7.713 s; and the time of multiple prediction and subtraction is 141 s. It takes a total of 210.6 s to calculate a shot. To save the computational source and the cumulative error of adaptive matching, Firstly, we superimposed all the predicted internal multiples and only use one adaptive subtraction to remove internal multiples from the original seismic data (Gu et al., 2023). However, some of the multiples information may be drowned out during normalization and addition. The accuracy of one-time multiple eliminations is not as high as that of layer-by-layer elimination. Therefore, in this study, we adopt the second method, but when dealing with other large amounts of seismic data, we can still use the first approach.

5. Conclusion

The elimination of internal multiples is a difficult problem in the field of seismic exploration data processing, particularly when dealing with field data from the northwest region of China. Most of the seismic data in this region are acquired using 3D geometry. In this study, we present the theory and application of the autofocusing Marchenko method on 3D seismic data. The Marchenko schemes can obtain Green's functions by creating virtual sources and receivers at any desired depth level. Therefore, this method can be employed to construct internal multiples at any interface. A multichannel adaptive filter is utilized to guarantee the thorough and accurate elimination of these predicted multiples. The approach fully considers the actual subsurface conditions and can effectively eliminate internal multiples in 3D seismic data. Additionally, the integration of Green's functions enables parallelization through pairs of focal points, rendering it particularly suitable for the application of large volumes of 3D seismic data. The application of both examples was successful and demonstrated the effectiveness of the 3D Marchenko method. Therefore, we conclude that the 3D Marchenko autofocusing method serves as an effective tool for predicting and removing of internal multiples from 3D seismic

CRediT authorship contribution statement

Pei-Nan Bao: Writing — original draft, Software, Methodology, Funding acquisition, Data curation. **Ying Shi:** Writing — review & editing, Supervision, Methodology. **Xin-Min Shang:** Supervision, Project administration, Data curation. **Hong-Xian Liang:** Validation, Supervision, Software. **Wei-Hong Wang:** Writing — review & editing, Visualization, Resources.

Declaration of competing interest

We declare that there is no conflict of interest exists in the submission of this manuscript, and the manuscript is approved by all authors for publication. I would like to declare on behalf of my co-authors that the work described was original research that has not been published previously, and not under consideration for publication elsewhere, in whole or in part, the manuscript entitled "Three-dimensional internal multiple elimination in complex structures using Marchenko autofocusing theory".

References

Bao, P., Wang, X., Xie, J., et al., 2021. Internal multiple suppression method based on iterative inversion. Chin. J. Geophys. 64 (6), 2061–2072. https://doi.org/ 10.6038/cjg202100285 (in Chinese).

Bao, P., Shi, Y., Wang, W., et al., 2022. An improved method for internal multiple elimination using the theory of virtual events. Petrol. Sci. 19 (6), 2663–2674.

https://doi.org/10.1016/j.petsci.2022.05.021.

- Baumstein, A., Hadidi, M.T., 2006. 3D surface-related multiple elimination: data reconstruction and application to field data. Geophysics 71 (3), E25–E33. https://doi.org/10.1190/1.2194515.
- Brackenhoff, J., Thorbecke, J., Meles, G.K., et al., 2022. 3D Marchenko applications: implementation and examples. Geophys. Prospect. 70 (1), 35–36. https://doi.org/10.1111/1365-2478.13151.
- Da Costa Filho, C.A., Meles, G.A., Curtis, A., 2017. Imaging with Marchenko focusing functions in acoustic and elastic media. In: 15th International Congress of the Brazilian Geophysical Society.
- Dragoset, B., Verschuur, E., Moore, I., et al., 2010. A perspective on 3D surface-related multiple elimination. Geophysics 75 (5), A245–A261. https://doi.org/10.1190/1.3475413.
- Elison, P., Dukalski, M.S., Devos, K., et al., 2020. Data-driven control over short-period internal multiples in media with a horizontally layered overburden. Geophys. J. Int. 221 (2), 769–787. https://doi.org/10.1093/gji/ggaa020.
- Gan, L.D., Xiao, F.S., Dai, X.F., et al., 2018. Breakthrough and significance of technology on internal multiple recognition and suppression: a case study of Ordovician Dengying Formation in Central Sichuan Basin, SW China. Petrol. Explor. Dev. 45 (6), 1023–1035. https://doi.org/10.1016/S1876-3804(18)30106-
- Gu, Z.W., Geng, J.H., Wu, R.S., 2023. An application of internal multiple prediction and primary reflection retrieval to salt structures. Geophysics 88 (6), S189—S201. https://doi.org/10.1190/geo2022-0669.1.
- He, W., Geng, J., 2022. Elimination of free-surface-related multiples by combining Marchenko scheme and seismic interferometry. Geophysics 87 (3), Q1—Q14. https://doi.org/10.1190/geo2021-0246.1.
- Hokstad, K., Sollie, R., 2006. 3D surface-related multiple elimination using parabolic sparse inversion. Geophysics 71 (6), V145–V152. https://doi.org/10.1190/ 1.2345050.
- ljsseldijk, J.V., der Neut, V., Thorbecke, J., et al., 2022. Extracting small time-lapse traveltime changes in a reservoir using primaries and internal multiples after Marchenko-based target zone isolation. Geophysics 88 (2), R135—R143. https://doi.org/10.1190/geo2022-0227.1.
- Ikelle, L.T., 2006. A construct of internal multiples from surface data only: the concept of virtual seismic events. Geophys. J. Int. 164 (2), 383–393. https:// doi.org/10.1111/j.1363-3246x.2006.02857.x.
- Jia, X., Zhao, Y., Snieder, R., 2019. Data interpolation for 3D Marchenko Green's function retrieval. SEG Technical Program Expanded Abstracts, pp. 4725–4729. https://doi.org/10.1190/segam2019-3216672.1.
- Kelamis, P., Verschuur, D., 2000. Surface-related multiple elimination on land seismic data—Strategies via case studies. Geophysics 65 (3), 719–734. https:// doi.org/10.1190/1.1444771.
- Meles, C.A., Löer, K., Ravasi, M., et al., 2015. Internal multiple prediction and removal using Marchenko autofocusing and seismic interferometry. Geophysics 80 (1), A7–A11. https://doi.org/10.1190/GEO2014-0408.1.
- Meles, G.A., Wapenaar, K., Curtis, A., 2016. Reconstructing the primary reflections in seismic data by Marchenko redatuming and convolutional interferometry. Geophysics 81 (2), Q15—Q26. https://doi.org/10.1190/GEO2015-0377.1.
- Mildner, C., Broggini, F., de Vos, K.J., et al., 2017. Source wavelet amplitude spectrum estimation using Marchenko Focusing Functions. In: 79th Annual International Conference and Exhibition, EAGE. Extended Abstracts.
- Panos, G.K., Verschuur, D.J., 2000. Surface-related multiple elimination on land seismic data-Strategies via case studies. Geophysics 65 (3), 719–734. https:// doi.org/10.1190/1.1444771.
- Peng, H., Dukalski, Marcin, Elison, P., et al., 2023. Data-driven suppression of short-period multiples from laterally varying thin-layered overburden structures. Geophysics 88 (2), V59–V73. https://doi.org/10.1190/geo2022-0241.1.
- Rose, J.H., 2002. 'Single-sided' autofocusing of sound in layered materials. Inverse Probl. 18 (6), 1923–1934. https://doi.org/10.1088/0266-5611/18/6/329.
- Singh, S., Snieder, R., Behura, J., et al., 2015. Marchenko imaging: Imaging with primaries, internal multiples, and free-surface multiples. Geophysics 80 (5), S165–S174. https://doi.org/10.1190/segam2014-1593.1.
- Slob, E., Wapenaar, K., Broggini, F., et al., 2014. Seismic reflector imaging using internal multiples with Marchenko-type equations. Geophysics 79 (2), S63–S76.

https://doi.org/10.1190/geo2013-0095.1.

- Staring, M., van der Neut, J., Wapenaar, K., 2018a. Marchenko redatuming by adaptive double-focusing on 2D and 3D field data of the Santos basin. SEG Technical Program Expanded Abstracts, pp. 5449–5453. https://doi.org/10.1190/segam2018-w4-02.1.
- Staring, M., Pereira, R., Douma, H., et al., 2018b. Source-receiver Marchenko redatuming on field data using an adaptive double-focusing method adaptive double focusing. Geophysics 83 (6), S579–S590. https://doi.org/10.1190/GE02017-0796.1.
- Staring, M., Dukalski, M., Belonosov, M., et al., 2021. Robust estimation of primaries by sparse inversion and Marchenko equation-based workflow for multiple suppression in the case of a shallow water layer and a complex overburden: A 2D case study in the Arabian Gulf. Geophysics 86 (2), Q15–Q25. https://doi.org/10.1190/geo2020-0204.1.
- Thorbecke, J., Zhang, L., Wapenaar, K., et al., 2021. Implementation of the Marchenko multiple elimination algorithm. Geophysics 86 (2), F9–F23. https://doi.org/10.1190/geo2020-0196.1.
- Thorbecke, J., Slob, E., Brackenhoff, J., et al., 2017. Implementation of the Marchenko method. Geophysics 82 (6), WB29—WB45. https://doi.org/10.1190/GEO2017-0108.1.
- Van der Neut, J., Wapenaar, K., 2016. Adaptive overburden elimination with the multidimensional Marchenko equation. Geophysics 81 (5), T265—T284. https:// doi.org/10.1190/GEO2016-0024.1.
- Wang, Y., 2003. Multiple subtraction using an expanded multichannel matching filter. Geophysics 68 (1), 354–364. https://doi.org/10.1190/1.1543220.
- Wapenaar, K., 2004. Retrieving the elastodynamic Green's function of an arbitrary inhomogeneous medium by cross correlation. Phys. Rev. Lett. 93 (25), 1–4. https://doi.org/10.1103/PhysRevLett.93.254301.
- Wapenaar, K., 2013. Three-dimensional Marchenko equation for Green's function retrieval "beyond seismic interferometry". In: SEG Houston 2013 Annual Meeting. https://doi.org/10.1190/segam2013-1005.1.
- Wapenaar, K., Thorbecke, J., Draganov, D., 2004. Relations between reflection and transmission responses of three-dimensional inhomogeneous media. Geophys. J. Roy. Astron. Soc. 156 (2), 179–194. https://doi.org/10.1111/jj.1363-3246X.2003.02152.x.
- Wapenaar, K., Broggini, F., Snieder, R., 2012. Creating a virtual source inside a medium from reflection data: heuristic derivation and stationary-phase analysis. Geophys. J. Int. 190 (2), 1020–1024. https://doi.org/10.1111/j.1363-3246X.2012.05551.x.
- Wapenaar, K., Broggini, F., Slob, E., et al., 2013. Three-dimensional single-sided Marchenko inverse scattering, data-driven focusing, green's function retrieval, and their mutual relations. Phys. Rev. Lett. 110 (8), 1–5. https://doi.org/10.1103/ PhysRevLett.110.084301.
- Wapenaar, K., Thorbecke, J., van der Neut, J., et al., 2014a. Green's function retrieval from reflection data, in absence of a receiver at the virtual source position. J. Acoust. Soc. Am. 135 (5), 2847–2861. https://doi.org/10.1121/1.4869083.
- Wapenaar, K., Thorbecke, J., van der Neut, J., et al., 2014b. Marchenko imaging. Geophysics 79 (3), WA39–WA57. https://doi.org/10.1190/geo2013-0302.1.
- Wapenaar, K., Brackenhoff, J., Marcin, D., et al., 2021. Marchenko redatuming, imaging, and multiple elimination and their mutual relations. Geophysics 86 (5), WC117—WC140. https://doi.org/10.1190/geo2020-0854.1.
- Weglein, A.B., Araújo, G.F., Carvalho, P.M., et al., 1997. An inverse-scattering series method for attenuating multiples in seismic reflection data. Geophysics 62 (6), 1975–1989. https://doi.org/10.1190/1.1444298.
- Zhang, L., Slob, E., 2019. Free-surface and internal multiple elimination in one step without adaptive subtraction. Geophysics 84 (1), A7–A11. https://doi.org/10.1190/geo2018-0548.1.
- Zhang, L., Slob, E., 2020. A field data example of Marchenko multiple elimination. Geophysics 85 (2), S65–S70. https://doi.org/10.1190/GEO2019-0327.1.
- Zhang, L., Staring, M., 2018. Marchenko scheme based internal multiple reflection elimination in acoustic wavefield. J. Appl. Geophys. 159, 429–433. https://doi.org/10.1016/j.jappgeo.2018.09.024.
- Zhang, L., Thorbecke, J., Wapenaar, K., et al., 2019. Transmission compensated primary reflection retrieval in the data domain and consequences for imaging. Geophysics 84 (4), Q27–Q36. https://doi.org/10.1190/geo2018-0340.1.